



Cite this: *Green Chem.*, 2021, **23**, 2628

Received 24th February 2021,  
 Accepted 12th March 2021

DOI: 10.1039/d1gc00711d

rsc.li/greenchem

## Gram-scale production of sugar nucleotides and their derivatives†

Shuang Li,<sup>‡a</sup> Shuaishuai Wang,<sup>‡b</sup> Yaqian Wang,<sup>a</sup> Jingyao Qu,<sup>c</sup> Xian-wei Liu,<sup>a</sup> Peng George Wang<sup>d</sup> and Junqiang Fang<sup>‡\*a</sup>

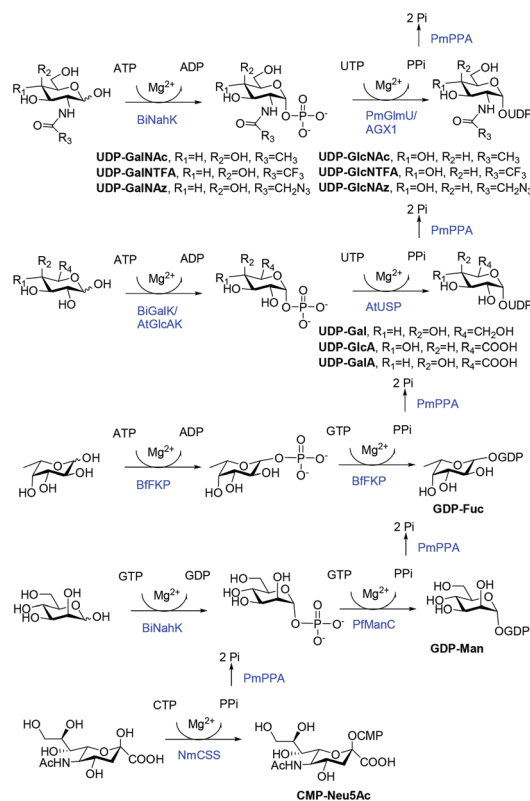
**Here, we report a practical sugar nucleotide production strategy that combined a high-concentrated multi-enzyme catalyzed reaction and a robust chromatography-free selective precipitation purification process. Twelve sugar nucleotides were synthesized on a gram scale with a purity up to 98%.**

Sugar nucleotides are essential intermediates for glycan metabolism and glycoconjugate biosynthesis.<sup>1</sup> They are formed as either nucleoside diphosphate (NDP) or monophosphate (NMP) nucleoside derivatives. In mammalian cells, only 9 common sugar nucleotides are used as essential donors for Leloir-type glycosyltransferases involved in most glycosylation reactions.<sup>2</sup> The affordable sugar nucleotides and their derivatives are one of the prerequisites for cell metabolic labeling and automated glycan synthesis.<sup>3–5</sup>

Chemical synthesis of sugar nucleotides has been well-documented. But low yield, tedious process and hazardous substances have restricted the application of this method.<sup>6,7</sup> In contrast, an enzyme-catalyzed synthetic reaction, which mimics the biosynthetic pathway, is considered more attractive with the advantages of strong regioselectivity and stereospecificity, high conversion rate, and mild reaction conditions.<sup>8</sup> Biosynthesis pathways of sugar nucleotides fall into two classes: *de novo* pathways and salvage pathways. In *de novo* pathways, sugar nucleotides are generated *via* multi-enzyme catalyzed reactions from monosaccharides or other sugar nucleotides, while in salvage pathways, sugar nucleotides are produced within 2 steps from monosaccharides *via* phos-

phorylation and subsequent pyrophosphorylation by one or two enzymes.<sup>9</sup> The salvage pathway (Scheme 1) has become the predominant approach for enzymatic synthesis of sugar nucleotides and their derivatives as fewer steps and enzymes are needed.<sup>10–14</sup>

Various strategies have been developed for the preparation of natural and unnatural sugar nucleotides, including chemical synthesis,<sup>6,15</sup> *in situ* regeneration,<sup>16,17</sup> one-pot multi-enzyme system,<sup>18,19</sup> metabolic engineering,<sup>20,21</sup> and super-



**Scheme 1** Common salvage synthetic routes to generate sugar nucleotides.

<sup>a</sup>National Glycoengineering Research Center, Shandong Provincial Key Laboratory of Glycochemistry and Glycobiology, Shandong University, Qingdao, Shandong 266237, People's Republic of China. E-mail: fangjunqiang@sdu.edu.cn

<sup>b</sup>Department of Chemistry, George State University, Atlanta, GA, 30302-4098, USA

<sup>c</sup>State Key Laboratory of Microbial Technology, Shandong University, Qingdao, Shandong 266237, People's Republic of China

<sup>d</sup>School of Medicine, Southern University of Science and Technology, Shenzhen, Guangdong 518055, People's Republic of China

†Electronic supplementary information (ESI) available. See DOI: 10.1039/d1gc00711d

‡These authors contributed equally to this work.

bead technologies.<sup>22</sup> However, a practical strategy is still unavailable due to two major bottlenecks: low substrate concentration of enzymatic reactions and time-consuming purification process. Most reported *in vitro* sugar nucleotide synthetic approaches are typically performed at substrate concentrations ranging from  $\mu\text{M}$  to 5–10 mM,<sup>10–14,16–19</sup> which lead to a huge reaction volume and extra chemical consumption once scaled up. Additionally, due to similarities of molecular weights and polar characteristics between products, substrates, and byproducts, the current purification processes mainly rely on chromatographic separation technologies, such as size exclusion chromatography, ion-exchange chromatography, or HPLC.<sup>23,24</sup> However, these methods could only be performed on a research scale in a time-consuming manner. Studies on glycans and glycoconjugates have been hindered by the lack of efficient strategies to produce substantial amounts of sugar nucleotides and their derivatives.

To accelerate applications of environmentally friendly enzymatic synthetic reactions and reduce waste accumulation, herein, we reported a practical and economical strategy for multi-gram scale production of sugar nucleotides (Scheme 2). With the employment of a high-concentrated multi-enzyme cascade synthetic system and a robust chromatography-free purification strategy, 12 sugar nucleotides and their derivatives were generated from cheap and readily available monosaccharides in a condensed reaction system with a starting monosaccharide up to 200 mM. More importantly, up to 2.35 g pure product could be obtained from a 20 mL reaction system by a selective precipitation process with a purity up to 98%. Subsequently, the synthesized sugar nucleotides were verified as glycosyl donors to generate the tumor-associated carbohydrate antigen, Globo H and its trifluoroacetyl modified derivative, in overall 85% yield *via in vitro* glycosyltransferase-catalyzed stepwise reactions.

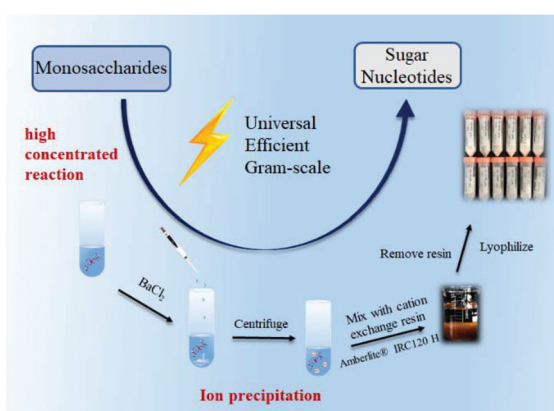
As mentioned above, the low substrate concentration of the enzymatic reaction system was unsuitable for practical applications. To improve the capabilities and efficiencies of the multi-enzymatic cascade reaction for sugar nucleotide pro-

duction, we first explored the optimal substrate concentration of the multi-enzymatic cascade reaction with high catalytic efficiencies. The salvage biosynthesis of UDP-GlcNAc was used for optimization and various substrate concentrations (5 mM, 10 mM, 50 mM, 100 mM, 200 mM and 300 mM) were assayed (Tables S1 and S2†). As depicted in Fig. S1,† the conversion rates were all above 90% when the concentration of GlcNAc was less than 200 mM ( $44.2 \text{ g L}^{-1}$ ). When the concentration reached 300 mM, the conversion rate decreased dramatically to 30%, leaving large amounts of unreacted GlcNAc. The low conversion rate may be due to the low fluidity of the reaction system, as reaction mixture containing 400 mM GlcNAc exhibited high viscosity, most likely hydrogel, leading to a low conversion rate. Thus, 200 mM was chosen as the optimal monosaccharide concentration. With the application of this high-concentrated multi-enzyme cascade reaction system, the synthetic reaction could be conducted in a mini tube with an improved space–time yield around 40 times when compared with the common 5 mM reaction system.

A buffer system, which functions to resist changes in the hydrogen ion concentration, has been extensively used in enzymatic reactions to mimic the biological environment. However, huge amounts of chemicals in buffer systems increase difficulties for product analysis and purification. To simplify the reaction system and facilitate the final purification process, we further evaluated the necessity of a buffer system for a high-concentrated enzymatic reaction system. Two enzymatic reactions with the same reactants for the synthesis of UDP-GlcNAc except the buffer system were carried out. As shown in Fig. S2,† the synthetic reaction without the buffer system could reach a comparable conversation rate to that with the buffer system, indicating that the effects of the buffer system could be omitted by pre-adjusting the pH value with the amounts of base solution directly, thus facilitating the subsequent purification process.

To reduce the cost-effectiveness, we also carried out the recovery of enzymes used for the synthesis of sugar nucleotides. The enzymes were recovered by ultrafiltration and reused for sugar nucleotide generation. As shown in Fig. S3,† the recovered enzymes could catalyze the completion of the reaction, which is consistent with a previous report.<sup>25</sup> However, a longer reaction time was needed when compared with the fresh enzymes, which may be due to the high-concentrated reaction system. Nevertheless, our results indicated that the enzymes used in this work can be recovered and could still catalyze the production of sugar nucleotides in high yields.

Having established the optimal reaction conditions for the synthesis of sugar nucleotides, we turned our efforts to explore an efficient strategy for the purification of sugar nucleotides. Challenges are multiplied when purifying the desired sugar nucleotides from a complex reaction mixture. Routine labor-intensive and time-consuming purification processes cannot guarantee large-scale purification under low-temperature conditions, thus may cause product degradation. Barium chloride precipitation<sup>26</sup> and silver nitrate precipitation<sup>27,28</sup> strategies have been reported for the purification of phosphate-contain-



**Scheme 2** A practical strategy for sugar nucleotide synthesis and purification on a multi-gram scale.

ing saccharides; however, the functions of metal ions in sugar nucleotide purification were not fully elucidated. Herein, seven metal ions ( $\text{Ag}^+$ ,  $\text{Ba}^{2+}$ ,  $\text{Cu}^{2+}$ ,  $\text{Zn}^{2+}$ ,  $\text{Ca}^{2+}$ ,  $\text{Mn}^{2+}$ , and  $\text{Ni}^{2+}$ ) that can undergo precipitation with phosphate ( $\text{PO}_4^{3-}$ ) were tested with a mixed solution containing ATP, UTP, and UDP-GlcNAc. As summarized in Fig. 1A,  $\text{Ag}^+$  and  $\text{Ba}^{2+}$  exhibited predominant efficiency than other metal ions. Subsequently, the selective precipitation abilities of  $\text{Ag}^+$  and  $\text{Ba}^{2+}$  toward nucleoside triphosphates (ATP, UTP, GTP, and CTP) were further measured. Both metal ions can precipitate nucleoside triphosphates with over 98% efficiency (Fig. 1B).

Additionally, recovery rates of two metal ions toward different sugar nucleotides were measured *via* the precipitation of pure sugar nucleotides with  $\text{Ag}^+$  and  $\text{Ba}^{2+}$ , respectively. UDP-GlcNAc, GDP-Fuc, and sugar nucleotides with carboxylic acid (UDP-GlcA, UDP-GalA and CMP-Neu5Ac) were assayed. As shown in Fig. 1C,  $\text{Ag}^+$  would precipitate sugar nucleotides with carboxylic acid, which would lead to a low recovery rate (20% to 40%), while  $\text{Ba}^{2+}$  gave over 95% recovery rate for all tested sugar nucleotides. It is worth mentioning that although  $\text{Ag}^+$  has been used for the purification of UDP-GlcNAc and its derivatives,<sup>29</sup> excess amount  $\text{Ag}^+$  needs to be removed immediately by NaCl precipitation and size exclusion chromatography due to its strong oxidizing properties, thus leading to more labor and low efficiency. Moreover,  $\text{Ag}^+$  cannot be used to precipitate carboxyl-containing structures, such as CMP-Neu5Ac and UDP-GlcA. Thus,  $\text{Ba}^{2+}$  was chosen as the optimal metal ion for the selective precipitation purification of sugar nucleotides.

To further investigate the mechanisms underlying  $\text{Ba}^{2+}$  precipitation, the composition of the formed precipitate was

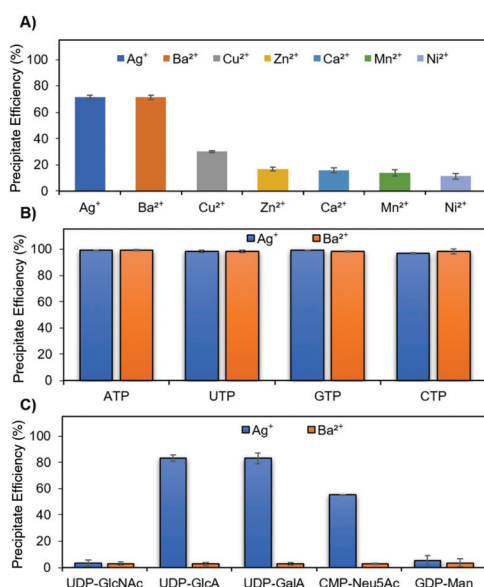


**Fig. 1** Evaluation of metal ions for the precipitation of sugar nucleotides. (A) Metal ions precipitate ATP, UTP and UDP-GlcNAc mixture solution; (B)  $\text{Ag}^+$  and  $\text{Ba}^{2+}$  precipitate nucleoside triphosphates; and (C)  $\text{Ag}^+$  and  $\text{Ba}^{2+}$  precipitate pure sugar nucleotides.

characterized by X-ray Photoelectron Spectroscopy (XPS). C 1s (284.8 eV) was used to calibrate the binding energies. Characteristic peaks of Ba, P, O and C elements were clearly observed in the full scan XPS spectra (Fig. 2A), which indicated that the precipitate contains the Ba element and corresponding nucleoside phosphates. The high resolution XPS spectrum of Ba 3d demonstrates that the binding energy of Ba in the precipitate complex has shifted from 0.5 eV to a lower value compared to that in  $\text{BaCl}_2$  (Fig. 2B), which indicated that electrons are transferred from Ba to the phosphate groups. These results imply that  $\text{Ba}^{2+}$  forms a coordinate covalent bond with a terminal phosphate in ATP and UTP (Fig. 2C). It is worth mentioning that two hydroxyl groups of the terminal phosphate and monosaccharide may play a critical role in the  $\text{Ba}^{2+}$  precipitation process as diphosphates on sugar nucleotides would not undergo precipitation with  $\text{Ba}^{2+}$ , while nucleoside triphosphates and nucleoside diphosphates could interact with  $\text{Ba}^{2+}$  to form precipitates. Furthermore, solid-state nuclear magnetic resonance ( $^{31}\text{P}$  ssNMR) was applied to verify the XPS results. As shown in Fig. 3A,  $^{31}\text{P}$  in the precipitate complex (ATP +  $\text{Ba}^{2+}$  or UTP +  $\text{Ba}^{2+}$ ) has shifted from 1.29 or 0.29 ppm to a high field compared to that in ATP or UTP (Fig. 3B), indicating that  $\text{Ba}^{2+}$  forms bonds with the phosphate group existing in the nucleoside triphosphates.

Finally, the practicability of the gram-scale sugar nucleotide synthetic strategy was systematically evaluated by the synthesis of 12 different sugar nucleotides and their derivatives in a 20 mL high-concentrated multi-enzyme cascade reaction, followed by the selective precipitation purification process. As shown in Table 1, the sugar nucleotide synthetic strategy developed in this study exhibited excellent yields up to 70–97% toward most sugar nucleotides except UDP-GalA. More importantly, 1.6–2.35 g final products with a purity up to 98% were quickly generated within 1 h *via* selective precipitation purification, demonstrating a powerful and robust separation protocol for glycobiological studies. It is worth mentioning that the

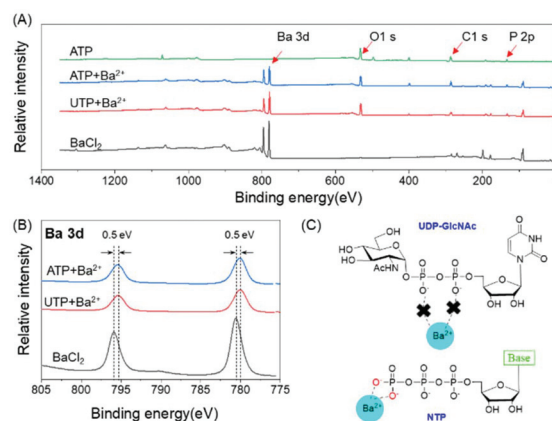


**Fig. 2** XPS measurements of  $\text{Ba}^{2+}$  precipitation. (A) Full scan XPS spectra of ATP, ATP +  $\text{Ba}^{2+}$ , UTP +  $\text{Ba}^{2+}$ , and  $\text{BaCl}_2$ ; (B) Ba 3d spectra of ATP +  $\text{Ba}^{2+}$ , UTP +  $\text{Ba}^{2+}$ , and  $\text{BaCl}_2$ ; and (C) the supposed mechanisms of  $\text{Ba}^{2+}$  precipitation.

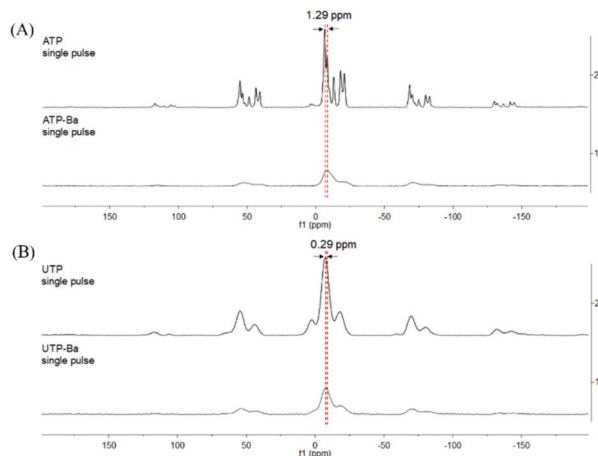


**Fig. 3**  $^{31}\text{P}$  ssNMR measurements of  $\text{Ba}^{2+}$  precipitation. (A)  $^{31}\text{P}$  ssNMR spectra of ATP and ATP +  $\text{Ba}^{2+}$  and (B)  $^{31}\text{P}$  ssNMR spectra of UTP and UTP +  $\text{Ba}^{2+}$ .

**Table 1** Gram-scale synthesis of sugar nucleotides and their derivatives via a high-concentrated multi-enzyme cascade synthetic system

Entry	Compound	Yield <sup>a</sup> (%)	Amount <sup>b</sup> (g)
1	UDP-GlcNAc	84	2.04
2	UDP-GalNAc	80	2.00
3	UDP-Gal	71	1.60
4	GDP-Fuc	68	1.60
5	GDP-Man	97	2.35
6	CMP-Neu5Ac	76	1.87
7	UDP-GlcA	69	1.62
8	UDP-GalA	52	1.23
9	UDP-GlcNTFA	78	2.06
10	UDP-GalNTFA	78	2.05
11	UDP-GlcNAz	81	2.10
12	UDP-GalNAz	79	2.05

<sup>a</sup> Yields calculated from the extracted product and theoretical amount.

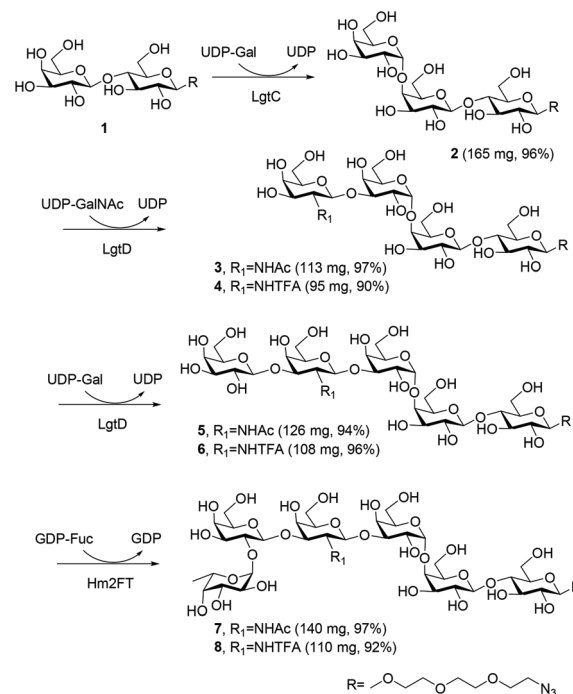
<sup>b</sup> Lyophilized pure product isolated from a 20 mL high-concentrated multi-enzyme cascade reaction system.

yield of UDP-GalA decreased to 52%, partly due to poor catalytic activities of BiGalK (galactokinase from *Bifidobacterium infantis*) and AtUSP (UDP-sugar pyrophosphorylase from *Arabidopsis thaliana*) toward the unnatural substrate GalA. All synthetic sugar nucleotides were well characterized by ESI-MS and NMR analysis, respectively (ESI<sup>†</sup>). Compared with the routine sugar nucleotide purification strategies, our method reduces environmental pollution as the reaction volume decreased significantly by using the high-concentrated enzymatic reaction. The whole processing time was also significantly reduced from 3–4 days to 1 day by the chromatography-free selective precipitation purification process.<sup>23</sup> Most importantly, as the existing technologies are not suitable for gram-scale production, our strategy has exceptional potential for sugar nucleotide production.

To verify the qualities of the formed sugar nucleotides, the amount of residual metal ions in the final products was measured by atomic absorption spectrometry (AAS) and induc-

tively coupled plasma mass spectrometry (ICP-MS). Sugar nucleotides were dissolved in a final concentration at  $30\ \mu\text{g mL}^{-1}$  using deionized water. The AAS results (Table S3<sup>†</sup>) showed that the concentration of  $\text{Na}^+$  is  $2.22\ \mu\text{g mL}^{-1}$ , indicating that UDP-GlcNAc binds to  $\text{Na}^+$  to form a disodium salt, and it failed to detect the concentrations of  $\text{Ba}^+$  and  $\text{Mg}^{2+}$ , as they were lower than the detection limit. ICP-MS (Table S4<sup>†</sup>) showed that the concentrations of  $\text{Ba}^{2+}$  and  $\text{Mg}^{2+}$  are  $44.77\ \text{ng mL}^{-1}$  and  $13.39\ \text{ng mL}^{-1}$ , respectively, which is equal to 0.14% and 0.04% (w:w), respectively. The trace amount of residual metal ions would not affect the subsequent usage as lower than 0.2% metal ion existed in sugar nucleotides.

Additionally, we explored the synthesis of the tumor-associated carbohydrate antigen Globo H (Fuc $\alpha$ 1-2Gal $\beta$ 1-3GalNAc $\beta$ 1-3Gal $\alpha$ 1-4Gal $\beta$ 1-4Glc), one of the most attractive biomarkers of cancer cells and cancer stem cells (Scheme 3).<sup>30</sup> Lactose  $\beta$ -PEG- $\text{N}_3$  was first extended with  $\alpha$ 1-4Gal using an  $\alpha$ 1-4-galactosyltransferase (LgtC)<sup>31</sup> in the presence of UDP-Gal. Then, the trisaccharide **2** was elongated by  $\beta$ 1-3GalNAc with the employment of UDP-GalNAc and  $\beta$ 1-3-*N*-acetylgalactosyl-transferase (LgtD) to afford compound **3**.<sup>32</sup> Interestingly, UDP-GalNTFA (UDP-*N*-trifluoroacetyl galactosamine), a C2 modified UDP-GalNAc analog, can also be recognized by LgtD to provide the tetrasaccharide derivative **4**. With the further extension of  $\beta$ 1-3-Gal by using LgtD and UDP-Gal to provide **5** and **6**, Globo H **7** (Fuc $\alpha$ 1-2Gal $\beta$ 1-3GalNAc $\beta$ 1-3Gal $\alpha$ 1-4Gal $\beta$ 1-4Glc $\beta$ -PEG- $\text{N}_3$ , 140 mg, 85% overall yield) and its derivative **8** (Fuc $\alpha$ 1-2Gal $\beta$ 1-3GalNAc $\beta$ 1-3Gal $\alpha$ 1-4Gal $\beta$ 1-4Glc $\beta$ -PEG- $\text{N}_3$ , 110 mg, 76% overall yield) were assembled by using GDP-Fuc and an  $\alpha$ 1-2-fucosyltransferase.<sup>33</sup> All synthesized compounds were con-



**Scheme 3** Stepwise synthesis of Globo H and its derivative.

firmed by ESI-MS and NMR analysis, respectively (ESI†). Compared to the assembly of Globo H by a sugar nucleotide regeneration system,<sup>32</sup> the synthesis of Globo H by using readily available sugar nucleotides simplifies the purification process and increases the overall yield, which provides a feasible way for the synthesis of oligosaccharides and their derivatives.

## Conclusions

Sugar nucleotides are essential intermediates involved in Leloir-type glycosyltransferase-catalyzed glycosylation processes. Current synthetic strategies are still facing several challenges, which in turn hinder the illustrations of biological roles of glycans and glycoconjugates. We herein reported a practical and economical approach toward the production of sugar nucleotides and their derivatives to meet the urgent needs in the large-scale synthesis of complex glycans and glycoconjugates. This universal approach could produce sugar nucleotides from the corresponding monosaccharides on a multi-gram scale with a combination of a high-concentrated multi-enzyme cascade reaction and a fast chromatography-free purification process. 12 kinds of sugar nucleotides and their derivatives were firstly synthesized on a multi-gram scale from a 20 mL reaction mixture and purified by a robust Ba<sup>2+</sup> selective precipitation process with a purity up to 98%. This methodology breaks through the limitations of existing strategies and provides new insights into the large-scale production of sugar nucleotides. The synthesized sugar nucleotides facilitate the *in vitro* synthesis of functional glycans, such as Globo H and its new derivative. Large-scale preparation of complex glycans and glycoconjugates employing this strategy is underway.

## Conflicts of interest

There are no conflicts to declare.

## Acknowledgements

This work was supported by the National Key Research and Development Program (2018YFA0901700), the National Science Foundation of China (31770854) and the Key Research and Development Program of Shandong Province (2019GSF107035).

## Notes and references

- L. L. Lairson, B. Henrissat, G. J. Davies and S. G. Withers, *Annu. Rev. Biochem.*, 2008, **77**, 521–555.
- A. Varki, R. D. Cummings, J. D. Esko, P. Stanley, G. W. Hart, M. Aebi, A. G. Darvill, T. Kinoshita, N. H. Packer and J. H. Prestegard, *Essentials of Glycobiology*, Cold Spring Harbor Laboratory Press, Cold Spring Harbor, New York, 3rd edn, 2015.
- P. Zhang, P. Liu, Y. Xu, Y. Liang, P. G. Wang and J. Cheng, *Carbohydr. Res.*, 2019, **472**, 72–75.
- J. Zhang, C. Chen, M. R. Gadi, C. Gibbons, Y. Guo, X. Cao, G. Edmunds, S. Wang, D. Liu, J. Yu, L. Wen and P. G. Wang, *Angew. Chem., Int. Ed.*, 2018, **57**, 16638–16642.
- Z. Liu, J. P. Li, M. Chen, M. Wu, Y. Shi, W. Li, J. R. Teijaro and P. Wu, *Cell*, 2020, **20**, 31245–31249.
- S. Ahmadipour and G. J. Miller, *Carbohydr. Res.*, 2017, **451**, 95–109.
- A. Miyagawa, S. Toyama, I. Ohmura, S. Miyazaki, T. Kamiya and H. Yamamura, *J. Org. Chem.*, 2020, **85**, 15645–15651.
- S. Ahmadipour, L. Beswick and G. J. Miller, *Carbohydr. Res.*, 2018, **469**, 38–47.
- M. Boyce, I. S. Carrico, A. S. Ganguli, S.-H. Yu, M. J. Hangauer, S. C. Hubbard, J. J. Kohler and C. R. Bertozzi, *Proc. Natl. Acad. Sci. U. S. A.*, 2011, **108**, 3141–3146.
- L. Cai, W. Guan, M. Kitaoka, J. Shen, C. Xia, W. Chen and P. G. Wang, *Chem. Commun.*, 2009, **20**, 2944–29446.
- L. Li, Y. Liu, Y. Wan, Y. Li, X. Chen, W. Zhao and P. G. Wang, *Org. Lett.*, 2013, **15**, 5528–5530.
- Y. Guo, J. Fang, T. Li, X. Li, C. Ma, X. Wang, P. G. Wang and L. Li, *Carbohydr. Res.*, 2015, **411**, 1–5.
- J. Liu, Y. Zou, W. Guan, Y. Zhai, M. Xue, L. Jin, X. Zhao, J. Dong, W. Wang, J. Shen, P. G. Wang and M. Chen, *Bioorg. Med. Chem. Lett.*, 2013, **23**, 3764–3768.
- Y. Li, H. Yu, H. Cao, S. Muthana and X. Chen, *Appl. Microbiol. Biotechnol.*, 2012, **93**, 2411–2423.
- G. K. Wagner, T. Pesnot and R. A. Field, *Nat. Prod. Rep.*, 2009, **26**, 1172–1194.
- C. H. Wong, S. L. Haynie and G. M. Whitesides, *J. Org. Chem.*, 1982, **47**, 5416–5418.
- T.-I. Tsai, H.-Y. Lee, S.-H. Chang, C.-H. Wang, Y.-C. Tu, Y.-C. Lin, D.-R. Hwang, C.-Y. Wu and C.-H. Wong, *J. Am. Chem. Soc.*, 2013, **135**, 14831–14839.
- H. Yu and X. Chen, *Org. Biomol. Chem.*, 2016, **14**, 2809–28018.
- S. Li, S. Wang, X. Fu, X. Liu, P. G. Wang and J. Fang, *Carbohydr. Polym.*, 2017, **178**, 221–227.
- K. Tabata, S. Koizumi, T. Endo and A. Ozaki, *Biotechnol. Lett.*, 2000, **22**, 479–483.
- Y. Zhai, D. Han, Y. Pan, S. Wang, J. Fang, P. Wang and X.-w. Liu, *Enzyme Microb. Technol.*, 2015, **69**, 38–45.
- X. Chen, J. Fang, J. Zhang, Z. Liu, J. Shao, P. Kowal, P. Andreana and P. G. Wang, *J. Am. Chem. Soc.*, 2001, **123**, 2081–2082.
- G. Zhao, W. Guan, L. Cai and P. G. Wang, *Nat. Protoc.*, 2010, **5**, 636–646.
- H. Eastwood, F. Xia, M. C. Lo, J. Zhou, J. B. Jordan, J. McCarter, W. W. Barnhart and K. H. Gahm, *J. Pharm. Biomed. Anal.*, 2015, **115**, 402–409.
- T. Fischöder, C. Wahl, C. Zerhusen and L. Elling, *Biotechnol. J.*, 2019, **14**, 1800386.
- C.-H. Wong, S. D. McCurry and G. M. Whitesides, *J. Am. Chem. Soc.*, 1980, **102**, 7938–7939.

- 27 L. Wen, K. Huang, M. Wei, J. Meisner, Y. Liu, K. Garner, L. Zang, X. Wang, X. Li, J. Fang, H. Zhang and P. G. Wang, *Angew. Chem., Int. Ed.*, 2015, **54**, 12654–12658.
- 28 L. Wen, K. Huang, Y. Liu and P. G. Wang, *ACS Catal.*, 2016, **6**, 1649–1654.
- 29 L. Wen, M. R. Gadi, Y. Zheng, C. Gibbons, S. M. Kondengaden, J. Zhang and P. G. Wang, *ACS Catal.*, 2018, **8**, 7659–7666.
- 30 S. J. Danishefsky, Y.-K. Shue, M. N. Chang and C.-H. Wong, *Acc. Chem. Res.*, 2015, **48**, 643–652.
- 31 J. Zhang, P. Kowal, J. Fang, P. Andreana and P. G. Wang, *Carbohydr. Res.*, 2002, **337**, 969–976.
- 32 J. Shao, J. Zhang, P. Kowal and P. G. Wang, *Appl. Environ. Microbiol.*, 2002, **68**, 5634–5640.
- 33 M. Li, X.-W. Liu, J. Shao, J. Shen, Q. Jia, W. Yi, J. K. Song, R. Woodward, C. S. Chow and P. G. Wang, *Biochem*, 2008, **47**, 378–387.